Paper No. 1180. (quote when citing this article)
Eleventh World Conference on Earthquake Engineering
ISBN: 0 08 042822 3

SOIL AMPLIFICATION AND SEISMIC MOTION OF SURFACE GEOLOGY INCLUDED PLEISTOCENE LAYERS IN HYOGOKEN-NANBU EARTHQUAKE

K. Sato, T. Kokusho, Y. Sawada and H. Yajima

Earthquake Engineering Department, Central Research Institute of Electric Power Industory
1646 Abiko, Abiko City, Chiba Prefecture, 270-11 Japan

ABSTRACT

During the 1995 Hyogoken-Nanbu Earthquake, strong acceleration records were obtained at several sites in and around Kobe city. At some of these recording sites, multi-level vertical arrays had to been installed, which demonstrated very peculiar nonlinear features of seismic amplification in reclaimed land areas and Holocene and Pleistocene deposits. The down-hole acceleration records on Port Island where one of the strongest accelerations was measured, have been analyzed with the inversion technique to estimate S-wave velocity and damping ratio corresponding to the main shock as well as a small aftershock. Records of three other down-hole sites with much different distances from the epicenter between them were also analyzed with the same technique. These studies disclosed effects of soil liquefaction and nonlinear soil properties on the peculiar seismic amplication mechanism at these sites.

KEYWARDS

Holocene; Pleistocene; S-wave velocity; Nonlinear; Inversion technique; Liquefaction.

INTRODUCTION

During the 1995 Hyogo-Ken Nanbu Earthquake (M_{JMA}=7.2), strong acceleration records with a maximum value of more than 0.8G (*n.b.*, G is the gravitational acceleration equal to 980 cm/sec^2) were obtaind at several sites in and around Kobe city in Japan. At some of the recording sites, multi-level vertical arrays had been installed, which demonstrated strong nonlinear features of seismic amplification in reclaimed land areas and also in and Holocene and Pleistocene soil layers. In this paper, the down-hole distribution of maximum accelerations is examined to discuss differences in non-linear amplification due to different intensity of input acceleration at the bottom of the vertical arrays. The record obtained at the Port Island site is analysed with "inversion technique" to compute from field data nonlinear soil properties based on recorded motions at different levels of the ground. The change in shear wave velocity and damping ratio for the mainshock are discussed from the viewpoint of liquefaction and strain-dependency. The same inversion analyses were applied at three other sites for various input accelerations in order to determine similar effects of soil nonlinearity.

ANALYSES OF THE EARTHUAKE RECORDS

Down-hole array sites

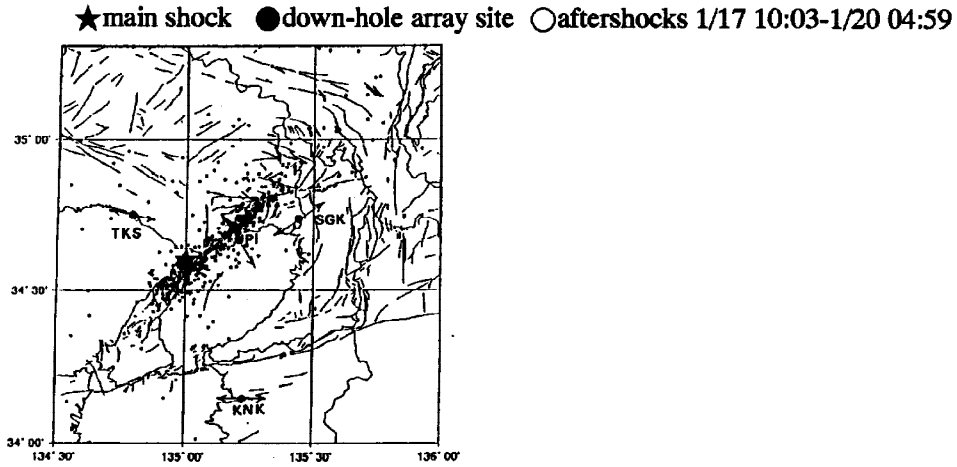

Fig.1. Location of down-hole array sites recorded around Osaka Bay and epicenters of the 1995 Hyogoken-Nanbu Earthquake (summarized by Disas. Prev. Res. Inst.)

Fig.1 shows the locations of four vertical array recording sites (designated PI, SGK, TKS and KNK) together with the epicenters of the main shock and many aftershocks which were summarized by the Disaster Prevension Research Institute of Kyoto University based on aftershock measurements carried out by a group of researchers. The aftershock epicenters may indicate the earthquke faults which were activated during the mainshock. The deepest level of the arrays ranged from -80 to -100m from the ground level at all four of the sites. The geological conditions at the deepest level are Pleistocene gravelly soils except for hard rock which exists at the KNK site. The upper layers consist of alternating Pleistocene gravel/clay layers, Holocene sand/clay layers and overlain by fill.

The horizontal orbits of the long-period particle motions for different levels at the four sites were obtained with a low-pass-filter of 0.2Hz. The principal axis of ground motion at each site is also shown. It was recognized that these directions comply with the source mechanism for a right-lateral slip fault. When original down-hole array records were analyzed, the following directional drift of buried seismometers were detected by these orbits for SGK, TKS and KNK motions (Sato *et al.*, 1995). Based on this information, the measurement data was properly adjusted for the angles hereafter except for PI where a 15 degree rotation was neglected because of small errors in the maximum acceleration of about 4%. The principal axis for all the points at each site have almost the same direction.

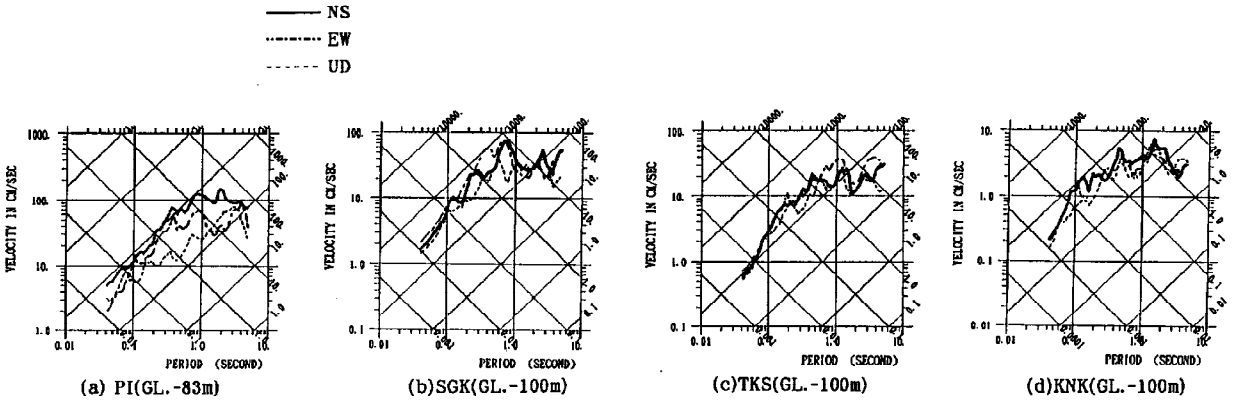

Fig.2 Pseudo velocity response spectra with damping ratio h=5%

Fig.2 indicates the pseudo velocity response spectra with a 5 % damping ratio in three directions for the observed motions at the deepest levels in the Pleistocene soil or hard rock at the four sites. The predominant periods of the motions in the horizontal directions are about 1.0 to 2.0 sec in PI, 0.6 to 0.7 sec in SGK, 1.0 sec in TKS, and 1.0 to 2.0 sec in KNK respectively. The corresponding maximum values of the amplitude indicate about 100 to 150 kine in PI, 80 kine in SGK, 40 kine in TKS, and 8 kine in KNK respectively. The values of the amplitude in the vertical direction are about 30 to 60 kine in PI, 40 kine in SGK, 20 kine in TKS, and 6 kine in KNK, respectively for about the same period as in the horizontal direction. The values of the spectral amplitude in the vertical direction therefore are nearly one half or less than one half of the respective maximum values in the horizontal direction except for the KNK site.

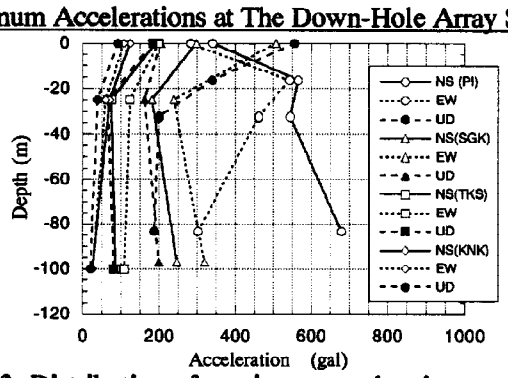

Fig.3. Distribution of maximum acceleration along the depth at the down-hole array sites

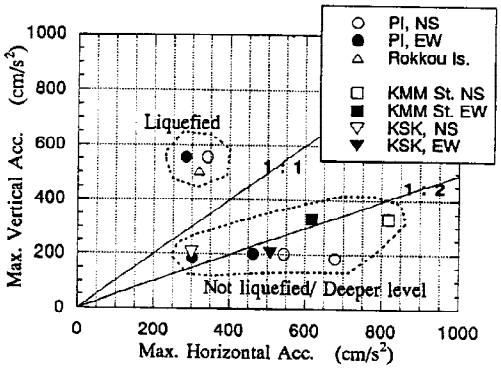

Fig.4. Relation of acceleration between vertical and horizontal direction

Fig.3 indicates the vertical distribution of maximum acceleration in two horizontal directions (NS,EW) and the vertical direction (UD) at the four sites.The maximum accelerations at the deepest level are different in a wide range(from 21gal in KNK to 679gal in PI) among the four sites with different distances from the epicenter, which may have led to noticeable differences in amplification characteristics in the upper soil layers. In the horizontal direction, the amplification between the ground surface and the deepest level was 4 to 5 times at KNK, while at TKS it was about 2 times for the acceleration of 100gal at the depth, whereas it was between 1 to 2 times for the acceleration of about 300gal in SGK and about one half in PI for the accelertions of 300 to 680gal. In PI, the surface sandy fill layer experienced very extensive liquefaction during the main-shock, which obviously led to the de-amplifcation of horizontal acceieration between the top and the bottom of the liquefied layer.

With regard to vertical acceleration, the amplification between the top and the bottom was 4.5 at KNK, 2 at TKS and unity at SKG, indicating an apparant downward trend of amplification with increasing acceleration at the bottom. In PI, however, it was as large as 3 times, implying that the amplification may not be dependent on only the intensity of acceleration. As a result, at PI the vertical acceleration at the surface was much higher than the horizontal.

Vertical maximum accelerations are plotted against horizontal maximum accelerations in Fig.4 for some sites where a horizontal acceleration of more than 300gal was recorded. Two straight lines drawn in the figure correspond to 1 to 1 and 1 to 2 slopes. Comparison of the plotted data with the lines discloses that the ratio between vertical and horizontal tend to be larger than unity for those sites where obvious liquefaction took place. The ratio seems to be around one half which has been considered normal for sites without liquefaction or at a deeper depth for the liquefied sites. It is therefore estimated that, at a liquefied site, horizontal motion tends to be greatly dampened while vertical motion is only slightly influenced by liquefaction while can still be amplified, resulting in a large vertical to horizontal acceleration ratio at the ground surface.

INVERSION TECHNIQUE

Inversion Analysis for PI Down-Hole Array Record

Geotechnical structure. This record was obtained from the Kobe City Municipal Office, who installed the down-hole array in the north-western part of the man-made island (PI). As shown in Fig.5, the top soil of the site is sandy fill (17.5m thick) called "Masa" (decomposesd granite transported from the nearby Rokko Mountains), underlain by Holocene soft clay and sand. These layers are underlain by alternative Pleistocene gravel and clay layers. Accelerometers in three directions were installed at four levels in the bore holes. The deepest one is located in a dense gravel layer with SPT blow-counts more than 60. P and S-wave velocities measured by means of down-hole seismic wave logging indicate that S-wave velocity (Vs) is about 200m/s at the top and 400m/s at the bottom while P-wave velocity (Vp) shows a big increase between the top (300m/s) and the bottom (2000m/s).

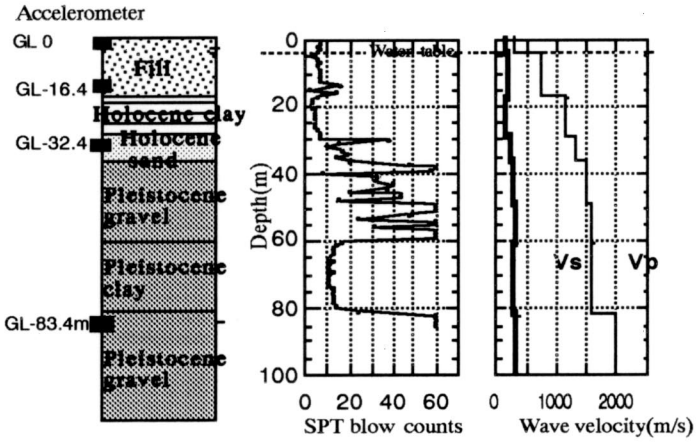

Fig.5. Geotechnical structure at the PI site

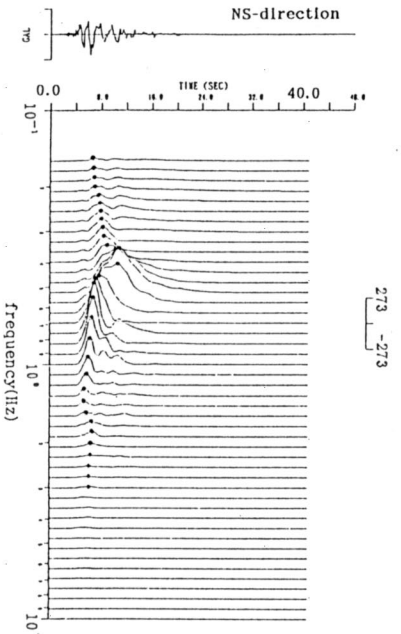

Fig.6. Evolutionary spectra (damping ratio h=5%) at PI (GL.0m) (see Kameda *et al.*, 1975)

Wave Motion Analysis. Fig.6 shows the evolutionary spectra (Kameda *et al.*, 1975) of the acceleration histories for NS components (GL.0m) at the ground surface level in PI, which were obtained by computing dynamic response anaysis for a one degree of freedom mass-model with a constant damping ratio due to the object motion. These spectra indicate the arrival time of the seismic wave and amplification with respect to the frequency and time. S-wave motions in both components consist of characteristic waves similar to two cycles of sinusoidal wave. Peaks of both spectra for the S-wave motion appear in the region of the frequency from 0.7Hz to 0.9Hz and concentrate in the time interval from 5.0 to 6.0 sec. The long-period peaks in NS component generated after the S-wave motion appear in the frequency less than 0.5Hz. Spectral peaks of the principal motion in the EW component also appear in the period slightly longer than NS component. For longer period waves it can be seen that the time for those peaks shifts in reverse proportion to the frequency less than 0.5Hz as shown with the dashed lines in Fig.6 indicating the dispersional characteristics of the surface waves.

Inversion Analysis. A computer code for the inversion analysis which was developed by Ohta(1975) and authors (Ishida *et al.* 1985) has been used in this study. In this case, multi-reflection of vertically propagating SH-wave in a horizontally layered system is assumed and the object function of the optimized problem is a transfer function of seismic motions between the ground surface and underground. In the analysis for horizontal motions, a layered soil model was assumed with soil density, shear wave velocity and damping ratio given by an initial estimate based on previous laboratory test results. Iteration with changing velocity and damping was then carried out to optimize best transfer functions between the ground surface and different buried accelerometer levels in order to reproduce the ones measured.

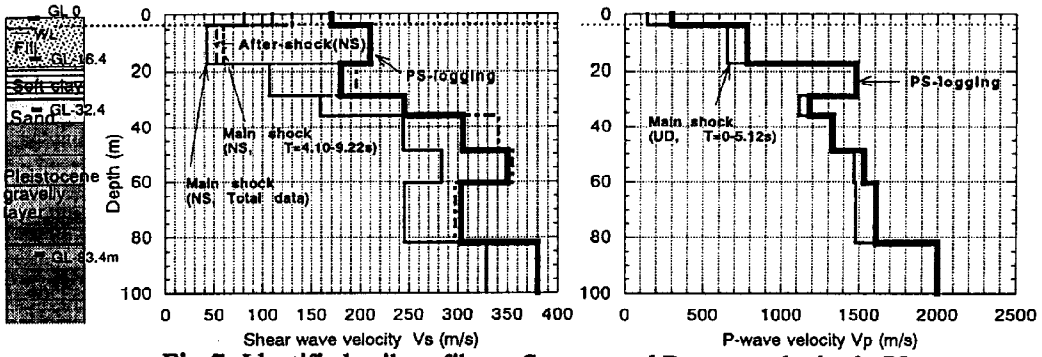

Fig.7. Identified soil profile on S-wave and P-wave velocity in PI

Fig.7 indicates the vertical variation of the optimized S and P wave velocities (Vs and Vp) in NS direction. The optimized Vs values for the total duration of the main-shock (T=20 seconds) were approximately 20% and 40% smaller than the initial values obtained by the PS-wave logging test for the Pleistocene and Holocene layer, respectively. For the fill layer, 80% and 50% reduction of Vs was identified for the saturated and unsaturated layers respectively, presumably because of the extensive liquefaction in the fill. In the same graph, Vs distribution optimized only for a part of the time (T=4.10 to 9.22 seconds) in which SH-wave is dominant in the measured time history as indicated in Fig.10 is shown. No meaningful difference can be seen between the results for the total time and the partial time except for the fill layer where the partial time analysis gives a smaller reduction of Vs implying that liquefaction was still developing during that time period.

Another interesting result was obtained from the analysis for one of the after-shocks with a maximum surface acceleration of about 10gal which occurred about two minutes after the main-shock. As shown in the graph, Vs for Pleistocene and Holocene layers can be interpreted to have returned to the initial value because of the small magnitude of the induced strain during the after-shock, while those in the fill layer take almost the same reduced value as the main-shock, indicating that the fill was still under a liquefied condition.

For the vertical acceleration, a similar inversion analysis was carried out based on the assumption that vertical seismic motion can be explained by the multi-reflection theory of vertically propagating P-wave. Fig.7 shows the result optimized for a time interval (T=0 to 5.12 seconds), in which P-wave motion looks most dominant. Despite some small difference of Vp from that of the PS-wave logging test, it may be concluded that the P-wave velocity changes little with the intensity of acceleration except for the unsaturated fill layer, where Vp is reduced by 50%. This result seems to confirm a theoretical basis of P-wave propagation through a saturated porous media in which no change in effective stress takes place.

Fig.8 shows damping ratio (h) for the NS horizontal motion optimized for the main shock and the aftershock. These vales are compared with the initial value estimated from previous laboratory test data for a small range of strain (Kokusho *et al.*, 1987). The optimized h for the after-shock is evidently larger than the respective laboratory test values by 5% for the Pleistocene soils and by 10 to 12% for the Holocene and fill layers. The same trend has also been pointed out in similar previous investigations (Kokusho *et al.*, 1992). For the main-shock, h is optimized as 6% for the Pleistocene soils and the Holocene sand layer and as high as 50% for the upper layer. Although the accuracy of the optimization for damping may not be so high, the equivalent damping ratio evaluated for a liquefied layer is very high.

Multi-reflection Analysis with Optimized Properties

Result for the PI. Fig.9 shows the vertical distribution of computed maximum acceleration in three directions to compare with those measured at four levels. The maximum difference between them is within 30%, and they seem to be consistent with each other both in quality and quantity. It can be readily understood from this figure that the previously mentioned vertical acceleration was great amplified, mainly due to the ground surface

at the upper boundary of the water table.

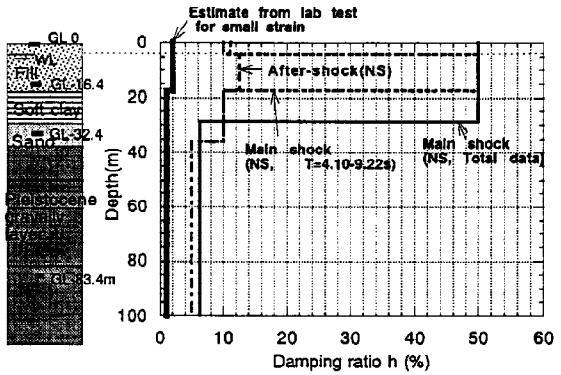

Fig.8. Identified soil profile on damping factor(h) of S-wave motion in PI

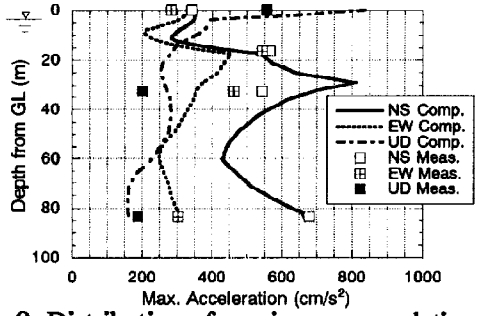

Fig.9. Distribution of maximum accerelation along the depth on both of analyzed and observed motion in PI

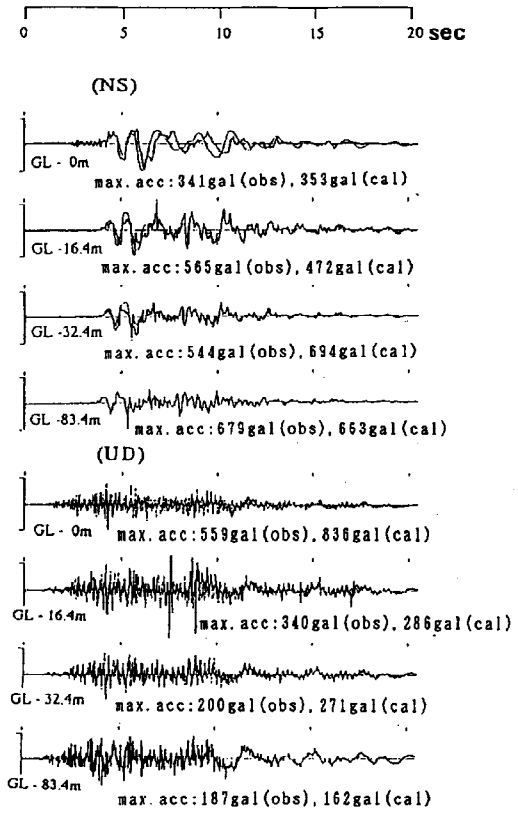

Fig.10. The accerelation time history of main shock in PI (observed motion ; bold line, analyzed motion ; broken line)

In Fig.10 wave motions of the main-shock in two directions measured at the four levels of PI-site are shown with thick lines. It can readily be seen that the vertical motion at GL-16.4m includes some spike-shape noises caused by some mechanical trouble. The maximum value of 340 gal can be read if the spike noise is filtered out. An ordinary multi-reflection analysis (Ohta *et al.*, 1975) of the main-shock was carried out on optimized soil properties to compare the results with measurements. Fig.10 shows the time histories for two directions at the upper three levels computed from the lowest levels, indicated with thin lines. The agreement between analysis and measurement is quite satisfactory for the horizontal motions at the middle two levels and also at the ground surface level, despite the fact that some visible phase lag was found in the measured wave compared to the analysis. The computed motions look smoother than the recorded ones, indicating that the analysis cannot fully reproduce higher frequency motions. For the vertical motion, the agreement is still good but in contrast with the horizontal motion, the analysis tends to exaggerate high frequency motions.

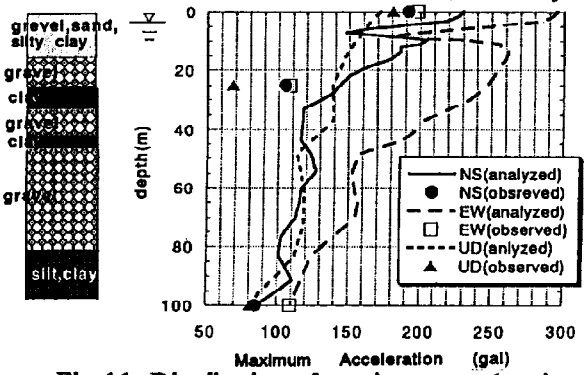

Fig.11. Distribution of maximum acceleration along the depth in SGK

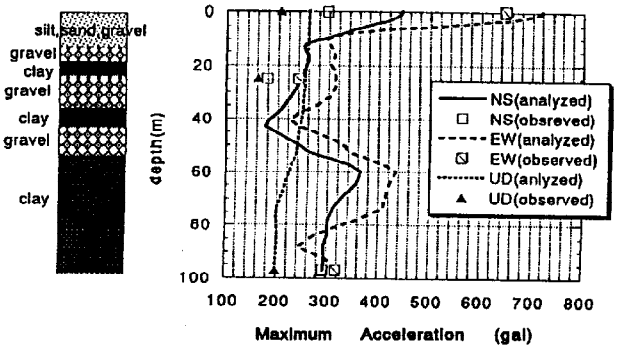

Fig.12. Distribution of maximum accerelation along the depth in TKS

Results for the other three sites. Results for SGK, TKS, and KNK were obtained by the same analysis method as discussed above. The optimized shear wave velocity (Vs) and P-wave velocity along the depth in NS, EW and UD directions are also computed for the three sites. The distribution of computed maximum acceleration in three directions with depth are similarly compared with the observed values for the three sites.

SGK is located very close to the source region of the activated faults but twice as far from the epicenter as PI. The optimized shear wave velocity (Vs) was approximately 25% and 45% smaller than the initial value for the Pleistocene and Holocene layer, respectively. Occurrence of liquefaction in the fill layer seems to have been neglected at this site based on no sand boils and no soil subsidence at the ground surface after the quake. The optimized P-wave velocity (Vp) changed very little from the initial value. Amplification of the horizontal acceleration through the Holocene and fill layers with sand and silt are most remarkable as seen in Fig.11.

Sand boils were observed after the quake, indicating that the soil liquefaction took place at TKS site. The optimized shear wave velocity (Vs) was approximately 10% and 30% smaller than the initial value for the Pleistocene and Holocene layer respectively. The optimized velocity of the sand layer at a depth of about GL.-10m is reduced by 80% from the initial value as in the liquefied fill layer in PI. This result also indicates the occurrence of liquefaction at this depth. Fig.12 indicates that de-amplification in the horizontal motion in the Holocene layer with sand and silt at the depth of 10m, seems to be affected by the onset of liquefaction. The computed acceleration is quite different with observed value at the level of GL.-25m. It may be difficult to simulate nonlinear seismic amplification using this multi-reflection analysis with optimized properties for such a long-duration time history as 20 seconds including completely different types of waves.

For the underlaying Pleistocene layers, the optimized value is evaluated to be nearly the same as the wave logging value, implying that strain-dependant variation in Vs is negligible in the Pleistocene layer for earthquake intensity experienced in KNK. The distribution of computed maximum acceleration with depth is compared with the observed value in three directions, indicating a striking agreement between them. It may be said that the analysis with the optimized properties could successfully reproduce the measured motions in KNK site mainly because the soils behaved basically linearly corresponding to moderate earthquake motion.

Comparion of transfer functions. Fig.13 show the amplificaion function between the ground surface level and the bottom level in the vertical-array at the four sites in the horizontal direction of EW component, respectively.

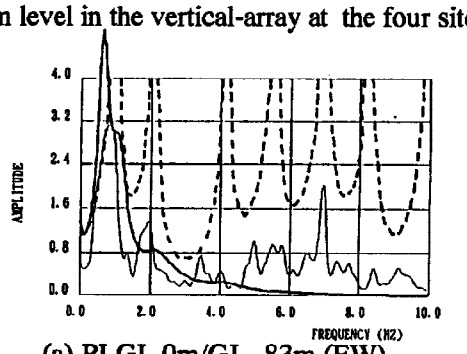

(a) PI GL.0m/GL.-83m (EW)

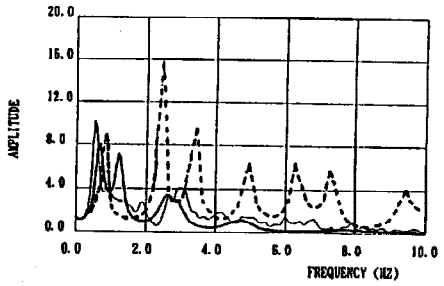

(b)SGK GL.0m/GL.-97m (EW)

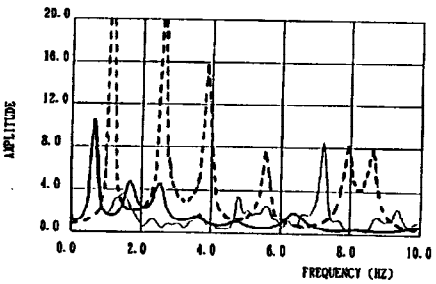

(c)TKS GL.0m/GL.-100m (EW)

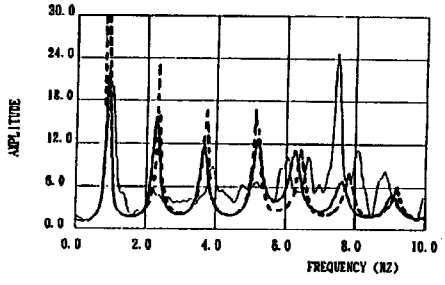

(d)KNK GL.0m/GL.-100m (EW)

Fig.13. Amplification function at the four sites (PS-log; dashed line, identified; bold line, observed; thin line)

The optimized amplifications obtained from the inversion analyses are indicated with bold lines in these figures, while the measured amplifications which were obtained from fourier spectral ratios between the ground surface and bottom levels are indicated with thin lines. The dashed line also drawn in the figure represents the transfer function computed for S-wave velocity corresponding to the PS-logging test.

The simulated and recorded ones are in very good agreement with each other, whereas the amplifications in the horizontal direction have sharp peaks of the first mode for all the four sites. The peaks appear at the frequency of 0.7 Hz in PI, 0.7 Hz also in SGK, 0.5 Hz in TKS, and 1.0 Hz in KNK. Those maximum values of the measured amplification for the mainshock are about 3.6 in PI, 10.0 in SGK, 10.0 in TKS, and 19.0 in KNK respectively. Taking into account the first natural frequencies corresponding to small strain wave velocity indicated in Fig.20 which are all about 1.0 Hz at the four sites, it is clearly demonstrated that the natural frequency for the mainshock is reduced to lower values than the initial due to a large strain-dependant variation of Vs at the three sites except for the KNK site. The amplification for the mainshock in PI is the smallest among the four sites, which indicates that the most extreme nonlinearity of soil including liquefaction took place there.

RESULTS

1) Seismic soil amplification in the horizontal direction was very variable with the input acceleration at the bottom level of the vertical arrays; In PI, with the base acceleration larger than 500 gals the acceleration was essentially de-amplified due to liquefaction and soil nonlinearity, whereas at KNK, with the base acceleration of 20～30 gals the acceleration was very much amplified.
2) The S-wave velocity optimized for the main shock was 40～45 % and 20～25 % smaller than initial values. for Holocene and Pleistocene soil layers in PI and SGK, both of which were near the focal area of the activated earthquake fault. In KNK the most remote from the focal area, the velocity reduction was found only 20 % for Holocene soils. The P-wave velocity optimized for the mainshock was essentially identical with the initial value at all sites based on PS logging tests, thus confirming the theoretical basis of P-wave propagation in a saturated porous media.
3) One-dimensional wave propagation analyses based on the optimized wave velocity successfully reproduced down-hole variations of maximum acceleration and acceleration time history at each level at most sites. The effect of soil liquefaction on the vertical change in maximum acceleration could be clearly shown at PI and TKS.
4) In terms of transfer fuctions, the analysis based on the optimized wave velocity could also reproduce the measured transfer functions with enough accuracy for engineering purposes. The peaks of transfer functions for horizontal response of the mainshock indicated a clear shift from those corresponding to initial wave velocity, and also indicated a large effect of soil nonlinearity.

References

Sato,K. and Kokusho,T. Matsumoto,M. Yamada,E. (1995). Nonlinearlity seismic response and soil property during strong motion. *Soil and Foundation Special Issue*.
Kameda,H. (1975). One technique to calculate evolutionary spectrum for strong motion. *JSCE*. **235**.
Ishida,K. Sato,K. Sawada,Y. and Yajima,H. (1985). Estimation of underground structure based on earthquake observation and normalized respons spectrum. *CRIEPI Report* . **385005**.
Kokusho,T. (1987). In-situ dynamic soil properties and their evaluations. *Proc. 8th Asian Regional Conference on soil Mechanics and Foundation Engineering*.
Kokusho,T., Tohma,J., Yajima,H., Tanaka,Y., Kanatani,M., and Yasuda,N. (1992). Seismic respones of soil layer and its dynamic properties. Proc. *10th World Conference on Earthquake Engineering*.
Ohta,H. (1975). Application of optimization method to earthquake engineering (Part 1)-Estimation of underqround structure of SMAC observation site in Hachinohe Harbor-. *Journal of Japan Society of Architectural Engineering* .